Influence of Anisotropy for the Characterization of Internal Imperfections in Pipes by Ultrasonic Non-Destructive Testing

Alejandra SEGURA[1,2], Patrick LANCELEUR[1], Jean-François DE BELLEVAL[1], Jean-Marc GHERBEZZA[1], Fréderic LESAGE[2]

[1] Laboratoire Roberval, Université de Technologie de Compiègne; Compiègne, France
Phone: +33 3 44234423, Fax: +33 3 44235287; e-mail: patrick.lanceleur@utc.fr, belleval@utc.fr, jean-marc.gherbezza@utc.fr
[2] Service de Contrôle Non Destructif, Centre de Recherche Vallourec, Aulnoye Aymeries, France
Phone: +33 3 27696695, Fax: +33 3 27674030; e-mail: alejandra.segura@vallourec.fr, frederic.lesage@vallourec.fr

Abstract
The Vallourec group is the world leader in seamless steel pipe manufacture for the oil and gas and energy sectors and for other industrial applications. With increasingly demanding customers and international standards, a number of quality inspections need to be implemented during production. One of these is ultrasonic testing, for which various technologies have been developed to make this inspection the most robust and the most reliable means of characterizing imperfections. One of the main limitations of these technologies is the lack of knowledge of the tensile properties of the materials and their variability from one part to another. These materials are considered to be isotropic although they can be slightly anisotropic. These anomalies may be connected to the various manufacturing processes (steel – product). The influence of the anisotropy of the materials inspected was therefore analyzed in order to estimate the precision of the algorithms defining the position and dimensions of the imperfections detected. For this, five samples of potentially anisotropic materials were tested in order to analyse their degree of anisotropy and their behaviour when interacting with an ultrasonic beam. This behaviour was analysed by means of an ultrasonic simulation model developed for this purpose.
Key words: Anisotropy, ultrasonic non-destructive testing, flaw dimensions and position, ultrasonic simulation.

1. Introduction

The Vallourec Group is the main producer worldwide of seamless steel pipes for various industrial applications. The main sectors of activity are centred around the oil and gas, engineering, petrochemicals, power generation and nuclear industries. These are all sectors where the quality requirements are extremely high. High technology non-destructive inspections must be implemented so as to meet the requirements of the standards and the customers.

Our research concerns the evaluation of the uncertainty of ultrasonic testing when estimating the dimensions and position of an imperfection in the internal skin of pipes made of various materials that are potentially anisotropic. A solid is anisotropic when its properties vary according to its orientation, for example if such a solid is subjected to tensile stress, the reaction will depend on the direction in which the stress was exerted. This effect can also be seen in ultrasonic wave propagation where there are variations in wave velocity according to the orientation of the anisotropic material.

Five materials were studied, three steels having been subjected to different heat treatments, one stainless steel (CRA – Corrosion Resistant Alloy) and one titanium. These materials were selected according to their possible degrees of anisotropy resulting from the various manufacturing processes used on the raw materials or on the finished product.

The dimension and position of the imperfections were estimated using a modelling tool developed specifically for this purpose. The inputs for this model are connected on the one hand to the characteristics of the anisotropic behaviour of the materials and on the other hand to those of the ultrasonic test used. As regards the outputs, two types of graph are available for making comparative analyses between the anisotropic case of each sample and the case of an equivalent isotropic material. It is thus possible to calculate the imperfection position and dimension errors.

2. The different sources of anisotropy and their origins in pipe manufacture.

A material may become anisotropic owing to different factors. These are particularly linked to crystallographic changes in the material. The main factors are as follows:

2.1. *Structure/texture anisotropy*

Structure anisotropy is due to variations in the crystalline orientation in the material. Experimental studies *[2], [3]* show the presence of alignments of grain axes oriented in a particular way in certain steels. This is the case of stainless steels, technically called *Corrosion Resistant Alloys* or *CRA*. Texture anisotropy is connected to the grain size. In the case of CRA steels, the smaller the wall thickness of the pipe, the finer the grains and the more accentuated the crystallographic orientation. This is also the case of titanium[1] which has a large grain size (around 100 microns). It also has a heterogeneous crystallographic texture which is hexagonal at low temperatures *[4]*. Plastic deformation of titanium results in random orientation of the grains, which can be a potential source of anisotropy. Plastic deformation modifies both the grain size and the crystalline orientation. We can therefore say that these two types of anisotropy are related.

2.2. *Composition anisotropy*

This type of anisotropy is mainly related to the contamination of the steel with such elements as aluminium, phosphorous, sulphur, manganese, etc. during the manufacturing process. When the steel bar is cooled in the continuous casting process, impure liquid solutions (containing the above elements) accumulate in certain zones. This phenomenon which is explained in *[5]* and *[6]* is technically known as segregation. This facilitates the weakening of the tensile properties and the appearance of cracks.

2.3. Stress anisotropy

This type of anisotropy is related to changes in the crystalline orientation owing to mechanical deformation. These deformations are essentially forming operations performed on the tube hollow after heat treatment. These operations involve plastic deformations with or without heating. The forming affects localized zones which generate residual stresses in the material, making it brittle and subject to cracking.

[1] Used for special applications: i.e. the aeronautics sector

3. Selection criteria for potentially anisotropic samples

Five samples were studied owing to their potential anisotropy of interest for our analysis. These were three samples of steel, one sample of CRA steel (stainless steel) and one sample of titanium. A description of their origin and composition is presented below.

BK: This is a steel tube hollow with out diameter (OD) 160 mm and wall thickness (WT) 10.325 mm having been subjected to cold drawing plastic deformations in two passes. A variation in dimension of 16.7% was observed. The potential anisotropy we have here is stress anisotropy.

E36 : This is a tube with the same grade, dimensions and plastic deformations as the BK tube, and which has, in addition, been heat treated. This heat treatment, called *Stress Relieving Heat Treatment* serves to remove stress and slightly modify the structure.

TG: This is a steel tube with 35 mm OD, 5 mm WT. This sample is interesting as it has followed all the plastic deformation operations and heat treatments, as well as a heavy drawing operation followed by straightening. Potential stress anisotropy may be present in this material.

Stainless Steel: This is an austenitic type CRA steel tube with 190.6 mm OD and 17.8 mm WT. Previous studies on this sample showed the grains to be highly elongated in the longitudinal direction of the tube, which produces potential structure anisotropy. The object of analysing this sample was to estimate the influence of this elongation.

Titanium: This is a titanium tube with 33.4 OD and 8.77 mm WT. It is a cold rolled biphasic material[2] which has the texture heterogeneities specific to titanium, such as those stated in the previous section.

4. Ultrasonic non-destructive testing of pipes and possible problems due to anisotropy

4.1. Ultrasonic non-destructive testing of pipes

Among the many ultrasonic testing techniques, it is the immersion technique that is the most suitable for pipes. It consists in immersing part of the pipe in a tank of water containing the ultrasonic probes. The pipe is, for example, rotated while the probe cell moves along the length of the pipe (Figure 2). In order to be able to represent the data, the position of the probe in relation to the pipe must be known either using an angle encoder, or by means of a laser system. This technique is much used industrially as it allows the entire pipe to be inspected automatically.

In order to give our study a focus, only longitudinal imperfections[3] located on the internal surface were taken into account. This type of imperfection was chosen mainly due to the fact that it is the most common type of flaw resulting from the manufacturing

[2] Made of aluminium and molybdenum.
[3] Elongated crack type flaws parallel to the pipe axis.

processes. The interpretation process involves estimating the seriousness of the flaws detected by determining their characteristics. One of the most representative characteristics of the seriousness of an imperfection is its depth, and it is therefore on this that we have focused our study.

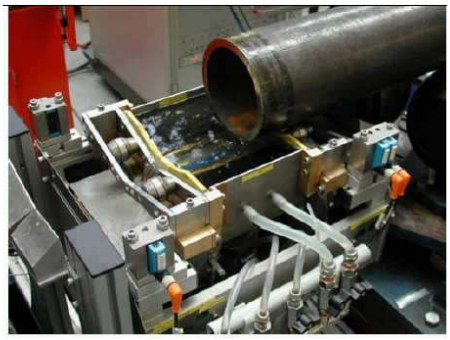

Figure 2 – Industrial ultrasonic testing bench for pipes

4.2. Interference with the ultrasonic response due to anisotropy

The main effect on the ultrasonic response caused by anisotropy is linked with the fact that the waves propagate in the material at velocities that vary according to the orientation in which they propagate. This phenomenon is described in detail in *[7]*. Contrary to the isotropic case, these waves, when transverse or longitudinal, have polarities that are neither purely transverse nor purely longitudinal. We call these quasi-transverse waves and quasi-longitudinal waves.

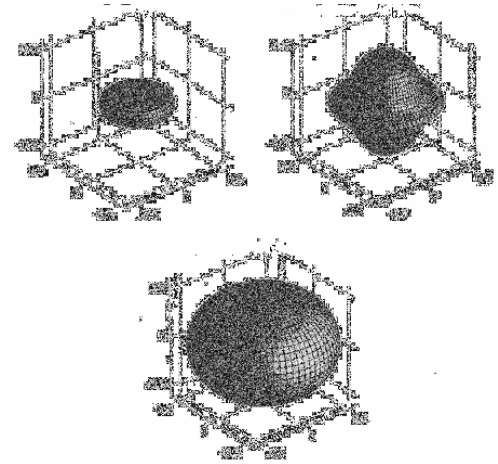

Figure 4 – Carbon-epoxy slowness surfaces. a. Quasi-longitudinal waves, b. Rapid quasi transverse waves, c. Slow quasi transverse waves. The three surfaces have a scale of s/km (source [7])

The variations in the wave propagation velocities are often represented using surfaces called slowness surfaces. These surfaces correspond to layers of points obtained by drawing from an origin a vector that is inversely proportional to the propagation velocity in the direction of this vector. In the case of isotropic media, these surfaces are spherical (radius independent from the direction), one of which corresponds to the longitudinal waves and the other to the transverse waves. This is no longer the case for

anisotropic materials, an example of which is given in figure 4 that corresponds to a carbon-epoxy composite[4]. In this case, there are three waves propagating in each direction, which means that the slowness surface is composed of the three layers represented in the figure.

5. Description of the tests

The five samples were cut as shown in Figure 5. The aim is to measure the time of flight of the ultrasonic wave propagation in several orientations and to deduce the speeds from the propagation distances.

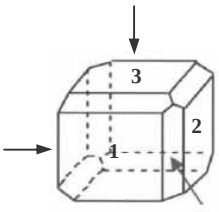

Figure 5 – Shape of cut samples

The time of flight of the longitudinal waves is measured by echography in immersion, marking the point where it passes through zero between the point of maximum amplitude and the point of minimum amplitude. For the transverse waves, the time of flight is measured by transmission[5] noting the point where it passes through zero between the point of maximum amplitude and the point of minimum amplitude on the first path. Three probes were used, one for longitudinal wave measurements and two (one emitting and one receiving) for transverse wave measurements. The longitudinal wave probe has a central frequency of 5 MHz and a diameter of 12.7 mm. The transverse wave probes have a central frequency of 2.25 MHz and a diameter of 12.7 mm. The time of flight measurements were made in 18 different configurations, taking into account the orientations represented in Figure 5 and the polarization of the waves (longitudinal and transverse horizontal and vertical).

6. Procedure for calculating elastic constants and slowness surfaces

Based on the time of flight measurements, the velocities were able to be deduced, owing to the fact that the thicknesses of the samples in each orientation were known. We were able to calculate the elastic constants in order to construct the anisotropic[6] and isotropic characterization matrix *[7]* . The anisotropic characterization matrix is written thus[7]:

[4] Carbon fibres embedded in an epoxy resin.
[5] Emission with one probe and reception with another probe.
[6] Said to be orthotropic as it is necessary to determine 9 independent elastic constants
[7] ρ corresponds to the volume density of the material.

$$[C_{ij}]=\begin{bmatrix} C_{11} & C_{12} & C_{13} & 0 & 0 & 0 \\ C_{21} & C_{22} & C_{23} & 0 & 0 & 0 \\ C_{31} & C_{32} & C_{33} & 0 & 0 & 0 \\ 0 & 0 & 0 & C_{44} & 0 & 0 \\ 0 & 0 & 0 & 0 & C_{55} & 0 \\ 0 & 0 & 0 & 0 & 0 & C_{66} \end{bmatrix},$$

$$C_{11} = \rho V_{11}^2$$
$$C_{22} = \rho V_{22}^2$$
$$C_{33} = \rho V_{33}^2$$
$$C_{44} = \rho V_{23}^2 = \rho V_{32}^2$$
$$C_{55} = \rho V_{13}^2 = \rho V_{31}^2$$
$$C_{66} = \rho V_{12}^2 = \rho V_{21}^2$$
$$C_{12} = \sqrt{(C_{11} + C_{66} - 2\rho V_{12/12}^2)(C_{22} + C_{66} - 2\rho V_{12/12}^2)} - C_{66}$$
$$C_{13} = \sqrt{(C_{11} + C_{55} - 2\rho V_{13/13}^2)(C_{33} + C_{55} - 2\rho V_{13/13}^2)} - C_{55}$$
$$C_{23} = \sqrt{(C_{22} + C_{44} - 2\rho V_{23/23}^2)(C_{33} + C_{44} - 2\rho V_{23/23}^2)} - C_{44}$$

The isotropic characterization matrix is reduced to two elastic constants c_{11} *and* c_{12}. c_{11} is calculated from the mean of constants $c_{11,}$ c_{22} and c_{33}. c_{12} is calculated from the means of constants $c_{44,}$ c_{55}, c_{66} and c_{11}. This matrix is written as follows:

$$c_{\alpha\beta} = \begin{pmatrix} c_{11} & c_{12} & c_{12} & 0 & 0 & 0 \\ c_{12} & c_{11} & c_{12} & 0 & 0 & 0 \\ c_{12} & c_{12} & c_{11} & 0 & 0 & 0 \\ 0 & 0 & 0 & \frac{c_{11}-c_{12}}{2} & 0 & 0 \\ 0 & 0 & 0 & 0 & \frac{c_{11}-c_{12}}{2} & 0 \\ 0 & 0 & 0 & 0 & 0 & \frac{c_{11}-c_{12}}{2} \end{pmatrix}$$

The elastic constants calculated in the isotropic and anisotropic case are presented in the following chart:

Table 1 – The elastic constants of the samples studied in the isotropic and anisotropic case

Elastic constants (GPa)	Sample														
	Titanium			E36			Stainless steel			BK			TG		
	Anisotopy	Isotropy	Absolute error	Anisotopy	Isotropy	Absolute error	Anisotopy	Isotropy	Absolute error	Anisotopy	Isotropy	Absolute error	Anisotopy	Isotropy	Absolute error
C11	164.139	169.730	5.591	275.956	276.301	0.345	258.406	258.783	0.377	271.095	272.079	0.984	281.958	283.155	1.197
C22	175.629			277.166			262.596			273.862			286.300		
C33	169.423			275.780			255.346			271.279			281.206		
C44	47.573			82.999			68.327			84.989			89.780		
C55	39.218			86.711			67.955			84.474			91.914		
C66	42.150	42.980	0.830	86.919	85.543	1.376	74.622	70.301	4.321	81.723	83.728	2.006	81.389	87.695	6.305
C12	84.093	83.770	0.323	106.356	105.214	1.142	99.284	118.180	18.896	121.084	104.622	16.462	113.054	107.766	5.288
C13	87.481			109.903			114.650			109.627			118.042		
C23	81.540			108.329			110.033			110.736			124.918		

By knowing the matrix in the anisotropic case, the slowness surfaces were able to be calculated for each sample. The slowness surfaces of the steels present a fairly low anisotropy, the most critical being material TG which has a slight variation at an angle of refraction of 45°, as this material is heavily drawn. Titanium and CRA (stainless steel) have a higher anisotropy than steels.

7. Estimation of the imperfection positioning and dimensioning error

This estimation is calculated using a digital simulator designed for this purpose. It simulates the propagation of an ultrasonic wave along a plane perpendicular to the generatrix of the tube in order to detect longitudinal imperfections. Two output representations are available, one regarding the position and the other regarding the

dimensions of the imperfections. The interpretation of each type of image is described at the end of this report.

Certain assumptions were made for the calculations. The ultrasonic beam is assimilated to the centre radius of the probe. This radius is placed at an angle of 17° in relation to the normal tube radial in order to obtain substantial propagation of transverse waves. The dimensions of the simulated tube are 100 mm OD and 5 mm WT. The flaw under consideration corresponds to a straight internal flaw 0.25 mm deep (5% of the WT).

The types of propagation modelled by the simulator correspond to those called “corner echoes” as illustrated in Figure 6, where the black arrows represent the incident wave and the red arrows the propagation in the material.

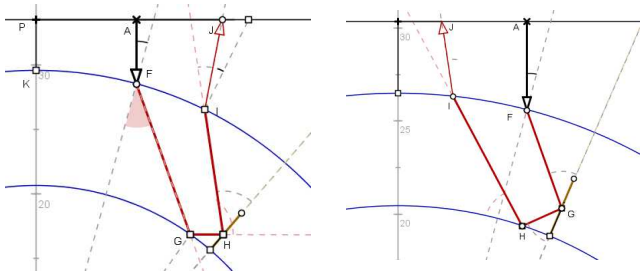

Figure 6 – “Corner echo” propagation type

7.1. Calculation of the positioning error

This calculation is based on a representation similar to the Bscan provided by the simulator, from which the amplitude data has been omitted. This representation shows the time of flight values according to the path of the ultrasonic probe. The time of flight corresponds to the path of the ultrasonic beam emitting and receiving transverse waves.

For each sample, two types of representation are obtained, one for the isotropic case and another for the anisotropic case. Each of these representations is obtained from the characterization matrices presented in the previous section.

These representations are analysed in order to extract the relevant data for comparing the ultrasonic responses obtained from the same imperfection in the two materials with similar characteristics, one anisotropic and the other isotropic. This data is as follows (Figure 7):

- Δt (µs): time interval related to the duration of the interaction of the ultrasonic beam with the imperfection,

- Δb (°): interval of the rotation positions (tube circumference) where the interaction of the ultrasonic beam with the imperfection occurred,

- (b, tv) = Centre point (scanning (°), time (µs)): point where the ultrasonic beam intercepts the edge of the imperfection emerging at the inner surface of the imperfection.

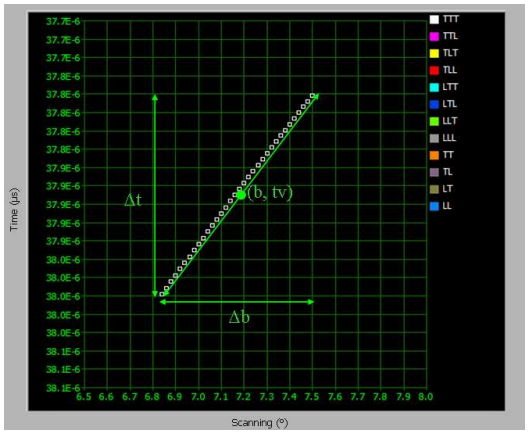

Figure 7 – Data analysed on the pseudo-Bscan

The error is calculated as the absolute difference between the previous data relating to the isotropic and anisotropic cases. The results are presented in the next section.

7.2. Calculation of the dimensioning error

The calculation is made on a simulated representation grouping the response in the isotropic and anisotropic cases (Figure 8). The x-axis of this representation corresponds to the scanning angle (as in a conventional Bscan) and the y-axis corresponds to the position in terms of depth of the place where the radius intersects with the imperfection. This graph is V-shaped, where each branch represents the interaction between the beam and the imperfection with both “corner echo” types of propagation illustrated in Figure 6.

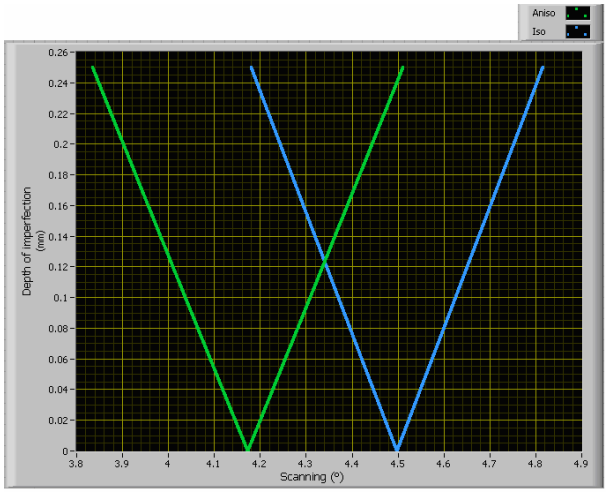

Figure 8 – Dimensioning graph: Depth of imperfection – Scanning angle. Blue line: isotropic case. Green line: anisotropic case.

Figure 9 explains the principle of the calculation. Conventionally, the dimension of an imperfection is interpreted by considering the material inspected to be isotropic (blue line). Point (B_{ip}, P_{ip}) corresponds to the point where the beam intercepts the imperfection at its maximum depth. With the anisotropic characterization, the curve moves and point (B_{ip}, P_{ip}) becomes (B_{ap}, P_{ap}). Supposing that the anisotropic characterization is not known and by analysing the experimental Bscans, we observe that the end of the segment related to the defect echo is in the angular position B_{ap}. The

projection (done blind, as the anisotropic curve is not known) of distance (B_{ac} - B_{ap}) on the isotropic curve (red line) arrives at a new point of interaction (B'_a, P'_a) on the depth of the imperfection, different to that on the original isotropic curve (B_{ip}, P_{ip}). The dimensioning error is thus the absolute difference between ordinates P_{ip} and P'_a.

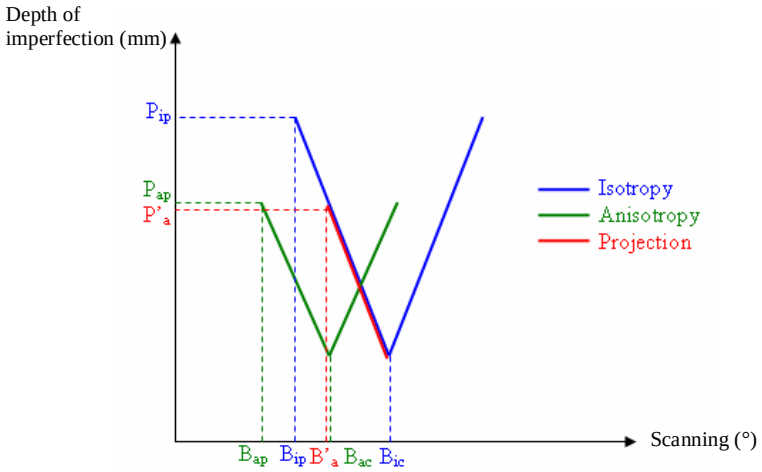

Figure 9 – Diagram explaining the calculation of the dimensioning error

These calculations are formulated as follows:

$$Dimensioning\ error = \left| P_{ip} - P'_a \right|$$

$$P'_a = f(B'_a)\ ;\ B'_a = B_{ic} - (B_{ac} - B_{ap})\ ;\ f : function\ of\ the\ isotropic\ characterization$$

8. Results of the influence of anisotropy on simulated Bscans

The results of the absolute positioning and dimensioning errors in the comparison between the isotropic and anisotropic cases on the five samples analysed are shown in Figure 10:

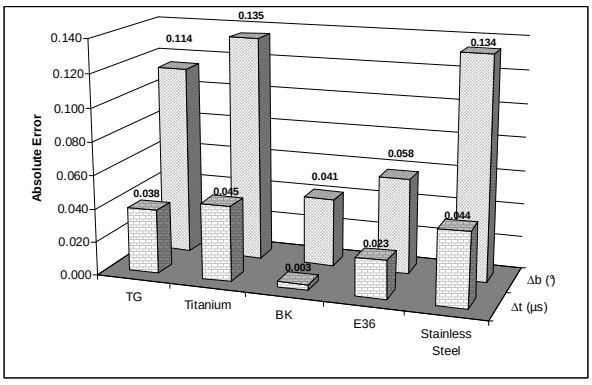

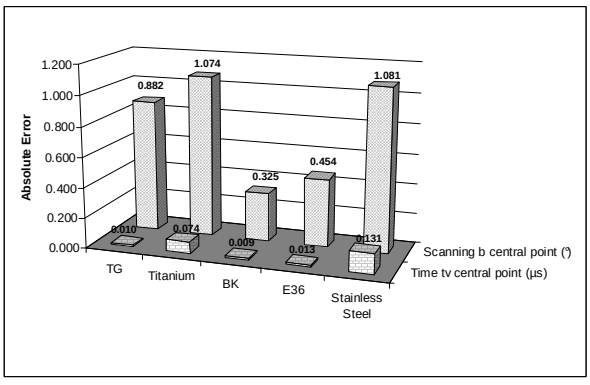

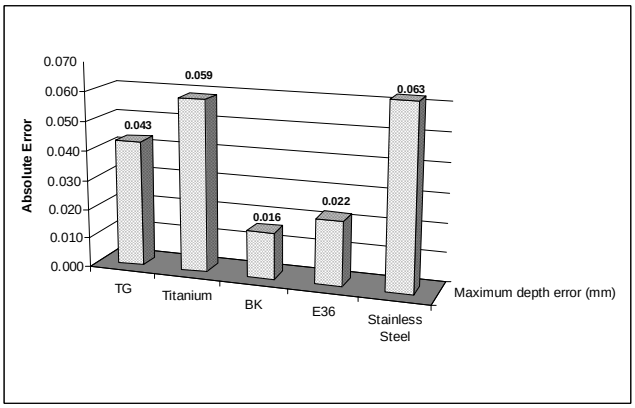

Figure 10 – Absolute errors – isotropic and anisotropic comparison of the five samples analysed

We can observe two groups: one containing materials TG, Titanium and Stainless Steel, where there is a considerable difference between the isotropic and anisotropic case for the positioning and dimensioning of imperfections. The other group contains steels BK and E36, where there is little difference between the isotropic and anisotropic case. In general, these dimensioning and positioning differences remain acceptable with regard to the required tolerances.

9. Conclusions

We may observe that it is structure/texture anisotropy that has the greatest influence in ultrasonic inspection for imperfection characterization, as seen in materials such as titanium and CRA (stainless) steel. In second position, we can say that stress anisotropy also has considerable influence, as seen in material steel TG which was subjected to high plastic deformations, mainly in the drawing process.

These results serve mainly to sensitize users of ultrasonic inspection techniques to the interpretation limits due to lack of knowledge of the tensile characteristics of the materials inspected. This aspect is not given much consideration industrially but is important for improving our knowledge of imperfections and their origins.

As a future improvement, we can extend this study to the different types of imperfections, taking into account reflection phenomena and mode conversions.

Acknowledgements

Michel Piette and the metallurgy team at the Vallourec Research Centre for their clear explanations of anisotropy, its types and its metallurgical phenomena. Marie-Christine Ho Ba Tho at the University of Technology of Compiègne for the equipment supplied for the tests.

References

[1] M. Dedieu, ‘Technologies du tube d’acier Vallourec’, September 1973.
[2] W. B. Hutchinson, K. Ushioda, G. Runnsjö, ‘Anisotropy of tensile behaviour in a duplex stainless steel sheet’. Materials Science and technology, Vol 1, September 1985.

[3] Mateo, L. Llanes, N. Akdut, J. Stolarz, M. Anglada, 'Anisotropy effects on the fatigue behaviour of rolled duplex stainless steels', International Journal of Fatigue, Vol 25. pp 481-488, 2003.
[4] 'Optimisation de la fabrication des tubes Titane par le procédé de laminage à pas de pèlerin', Thèse de E. Lenarduzzi – Université de Metz, France, Novembre 2005.
[5] Ghosh, 'Segregation in Cast Product', Sadhana, Vol. 26, parts 1 & 2. pp. 5-24, 2001.
[6] Garcia, J. Alvares, C. Dos Santos, N. Cheung, 'Lingotamiento Contínuo de Aços", São Paulo, Associaçao Brasileira de Metalugia e Materiais, 320 p, 2006.
[7] 'Matériaux et acoustique 1: propagation des ondes acoustiques 1', ed. by M. Bruneau, C. Potel, Lavoisier, 337 p, 2006.